불규칙 노면을 고려한 3차원 자동차 모델에 의한 강교의 동적 응답에 관한 연구

A Study on Traffic-Induced Vibration of Steel Girder-Bridge by Three-Dimensional Vehicle Model on Random Road Profile

김 철 우[1] · 川谷充郎[2] · 이 우 현[3]
Kim, Chul Woo Kawatani, Mitsuo Lee, Woo Hyun

요 약 : 橋梁의 動的應答을 파악하기 위해서는 路面조도에 의해 영향을 받는 차량의 거동 파악이 중요하게 된다. 최근, 교량의 床版등에서 발생되는 疲勞의 영향에 대한 관심이 고조되어 서서히 교통진동의 3차원 모델링에 대한 중요성이 대두되고 있다. 이에 본 연구에서는 교량에 발생되는 交通振動의 영향을 좀더 정확히 표현하기 위하여 3차원 해석방법을 제시한다.

해석방법으로 유한 요소법이 이용되었고, 차량 모델링은 하나의 前軸과 두 개의 後軸을 갖는 8自由度系 차량 모델을 이용하여 수치 시뮬레이션을 수행하였다. 動的 聯立微分方程式의 해법에서는 Newmark-β法을 이용하였고, 가상 노면凹凸모델링에서는 定常不規則過程으로 가정하여 노면 凹凸을 생성하여 시뮬레이션에 사용하였다. 또한 실제 차량 및 교량에서의 실측치와 비교하여 모델의 검증을 수행하였다.

핵 심 용 어 : 교통진동, 3차원 동적해석, 불규칙 노면凹凸, 동적증폭계수

1. Introduction

To investigate a traffic-induced vibration of bridges, especially those composed of short or medium span, it is very important to consider effects of vehicle motion coupled to bridge with random road roughness. Moreover in technical problems related to dynamic problem of short or medium span bridges, it becomes more important to understand the effect of vehicle, and the troubles such as fatigue that occurs in bridge deck or floor systems have been awakening interest in recent. Therefore in this study to solve those dynamic behavior of highway brid-

1) 중앙대학교 토목과 박사과정 수료, 일본 대판대학 연구원
2) 일본 대판대학 공학부 토목과 조교수
3) 중앙대학교 공과대학 토목공학과 교수

ges more accurately, three dimensional analytical method for traffic-induced vibrations of bridge is proposed. In addition there is another very important factor that should be accounted into traffic-induced vibration. It is the road surface roughness that has irregularities. Of course this research has considered its randomness by use of spectral analysis based on the researches which had been done by many researchers.[1~4]

In the numerical analysis, the strain of external girder is studied under several vehicle speed conditions and irregular road profiles that are randomly generated by Monte Carlo method with the variation of road profile spectrum model $S_z(\Omega)=\alpha/(\Omega^n+\beta^n)$. The effect of road surface roughness to dynamic response of bridge is studied. It can be seen that the variation of response between generated road profiles becomes gradually large according to spectral roughness coefficient α from the results of parametric study on spectrum of road profile.

To verify proposed analytical method, the analytical results are compared with those of experiment, and in this case measured road surface roughness is used.

2. Modeling of 3-dimensional F. E. M. bridge model

Generally speaking bridge is a structure composed of deck plate and girder system, therefore to express the bridge by analytical method of F. E. M it is common to make it up with plate and beam elements. In this paper by using these concepts, a numerical bridge model is constructed.

2.1 Stiffness matrix of plate element

The plate element used in this study is similar to that of general F. E. M. or plate theory, so that it can be considered as in-plane action in addition to out-of-plane action like as shown in Fig. 1.

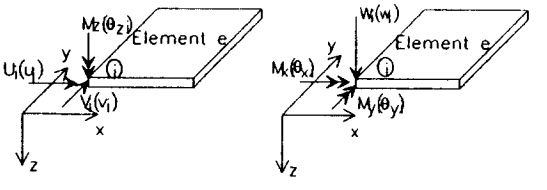

(a) in-plane action (b) out-of-plane action

FIG. 1 Plate Element

The matrix formation of in-plane action in Fig. 1(a) can be expressed as follows:

$$\{F_{inp}\} = [K_{inp}]_i \{a_{inp}\}_i \tag{1}$$

where, $\{a_{inp}\}_i = \begin{pmatrix} u_i \\ v_i \end{pmatrix}$, $\{F_{inp}\}_i = \begin{pmatrix} U_i \\ V_i \end{pmatrix}$

and the term about θ_{zi} may be neglectable because its effect to in-plane action will be very small. Of course by assuming θ_{zi} to be zero, it is apparent for the matrix to become singular. However within the whole matrix of bridge model, the stiffness matrix of beam element compensates this singularity. In the case of out-of-plane action, the matrix formation may form a well known formation as shown in Eq. (2). Additionally the behavior between in-plane and out-of-plane action is independent of each other, so that it may be treated as used in this paper :

$$\{F_{outp}\}_i = [K_{outp}]_i \{a_{outp}\}_i \quad (2)$$

where, $\{a_{outp}\}_i = \begin{Bmatrix} w_i \\ \theta_{xi} \\ \theta_{yi} \end{Bmatrix}$, $\{F_{outp}\}_i = \begin{Bmatrix} W_i \\ M_{xi} \\ M_{yi} \end{Bmatrix}$

Equation (3) is the united formation of Eq. (1) and Eq.(2), and finally it becomes the stiffness matrix of plate used in this paper:

$$\{F\}_i = [K]_i \{a\}_i \quad (3)$$

where, $\{a\}_i = \begin{Bmatrix} w_i \\ v_i \\ u_i \\ \theta_{xi} \\ \theta_{yi} \\ \theta_{zi} \end{Bmatrix}$, $\{F\}_i = \begin{Bmatrix} U_i \\ V_i \\ W_i \\ M_{xi} \\ M_{yi} \\ M_{zi} \end{Bmatrix}$,

$$[K]_i = \begin{bmatrix} [K_{inp}]_i & [0] \\ [0] & [K_{outp}]_i \end{bmatrix}$$

2.2 Stiffness matrix of beam element

A stiffness matrix of beam element that has six degrees of freedom at each node is generally used in structural engineering and so that derivation is omitted in this paper but the final formation becomes as Eq.(4):

$$\{F\}_{beam} = [K]_{beam}\{a\}_{beam} \quad (4)$$

where,

$$\{F\}_{beam} = \{F_{xi}, F_{yi}, F_{zi}, M_{xi}, M_{yi}, M_{zi}, F_{xj}, F_{yj}, F_{zj}, M_{xj}, M_{yj}, M_{zj}\}$$

$$\{a\}_{beam} = \{u_i, v_i, w_i, v_i', u_i', \theta_i, u_j, v_j, w_j, v_j', u_j', \theta_j\}$$

2.3 Mass matrix of plate element

A mass matrix of plate used in this paper is treated as lumped mass. The mass of an element is divided into four and lumped it at each node. The mass matrix of plate element is shown in Eq.(5) and m expresses a mass of plate element:

$$[M]_{plate} = \frac{m}{4} \begin{vmatrix} 1 & & & & & & & & & & & \\ & 1 & & & & & & & & & & \\ & & 1 & & & & & & & & & \\ & & & 1 & & & & & 0 & & & \\ & & & & 1 & & & & & & & \\ & & & & & 1 & & & & & & \\ & & & & & & 1 & & & & & \\ & & & & & & & 1 & & & & \\ & & & 0 & & & & & 1 & & & \\ & & & & & & & & & 1 & & \\ & & & & & & & & & & 1 & \\ & & & & & & & & & & & 1 \end{vmatrix} \quad (5)$$

2.4 Mass matrix of beam element

A mass matrix of beam is modeled by means of consistent-mass method and the matrix formation is as follows:

$$[M_{axial}] = \frac{\gamma Al}{6} \begin{bmatrix} 2 & 1 \\ 1 & 2 \end{bmatrix} \quad (6)$$

$$[M_{flex}] = \gamma \frac{Al}{420} \begin{bmatrix} 156 & & SYM. & \\ 22l & 4l^2 & & \\ 56 & 13l & 156 & \\ -13l & -3l^2 & -22l & 4l \end{bmatrix} \quad (7)$$

$$[M_{torsion}] = \frac{\gamma Alr_0^2}{6} \begin{bmatrix} 2 & 1 \\ 1 & 2 \end{bmatrix} \quad (8)$$

where, γ : *Density*(t/m^3)

J : *torsional rigidity*

$r_0^2 : J/A$

2.5 Damping matrix characteristics[5)]

A method adopted in this research to estimate a structural damping of bridge is by taking the damping matrix proportional to both the mass and stiffness matrices like as follows:

$$\Phi^T C_b \Phi = p\Phi^T M_b \Phi + q\Phi^T K_b \Phi \tag{9}$$

where p and q are constants obtained by solving the two simultaneous equations resulting by specifying the damping ratios β_1 and β_2 in two modes of vibration with natural circular frequencies ω_1 and ω_2. Φ is mode matrix, C_b is damping matrix, M_b is mass matrix and K_b is stiffness matrix of a bridge. Using the first two modes the constants are given by,

$$p = \frac{2\omega_1\omega_2(\beta_1\omega_2 - \beta_2\omega_1)}{\omega_2^2 - \omega_1^2} \tag{10}$$

$$q = \frac{2(\beta_2\omega_2 - \beta_1\omega_1)}{\omega_2^2 - \omega_1^2}$$

The values of the damping ratio at the higher modes can then be determined by

$$\beta_i = \frac{p + q\,\omega_i^2}{2\omega_i} \tag{11}$$

In this case first two fundamental frequencies of the structure need to be known, therefore, these frequencies are obtained from the solutions of eigen value problem.

3. Modeling of 3-dimensional vehicle model[8)]

To construct dynamic equations of bridge and vehicle models which are coupled reciprocally, first of all it is necessary to formulate equations of 3-dimensional vehicle model. Procedures of formation of an 8-degree-of-freedom vehicle model are to be composed of three parts: 1) to build dynamic equations about upper part of suspension, 2) to build dynamic equations about lower part of suspension or tires and finally 3) to construct entire equations of vehicle in relation to road surface roughness. After obtaining vehicle equation of motion it is possible to link them with those of bridge model.

Figure 2 shows a 8-degree-of-freedom vehicle model. In Fig. 2 m expresses mass, k stiffness, c damping coefficient.

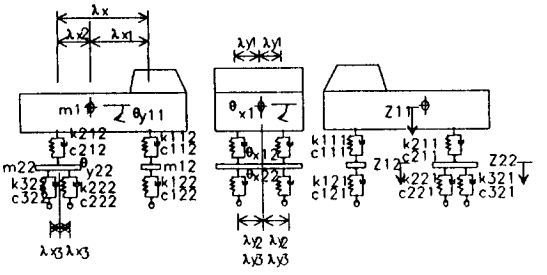

FIG. 2 Idealized vehicle model

By using the Lagrange equation of motion as shown in Eq. (12), it is possible to derive the equations of motion about an idealized vehicle model.

$$\frac{\partial}{\partial t}\left(\frac{\partial T}{\partial q_k}\right) - \frac{\partial T}{\partial q_k} + \frac{\partial U_e}{\partial q_k} + \frac{\partial U_d}{\partial q_k} = 0 \tag{12}$$

where, T ; Kinematic energy

U_e ; Position energy by elastic motion

U_d ; Dissipation energy by damping

Equations of vehicle motion become Eq.(13) ~(20) by using the concept of Eq.(12).

$$m_{v11}\ddot{z}_{11} + \sum_{s=1}^{2}\sum_{u=1}^{2} v_{s1u}(t) = 0 \tag{13}$$

$$m_{v11}\lambda_{x1}\lambda_{x2}\ddot{\theta}_{y11} - \sum_{s=1}^{2}\sum_{u=1}^{2}(-1)^s\lambda_{xs}v_{s1u(t)} = 0 \tag{14}$$

$$m_{v11}\lambda_{y1}{}^2\ddot{\theta}_{x11} + \sum_{s=1}^{2}\sum_{u=1}^{2}(-1)^u\lambda_{ys}v_{s1u(t)} = 0 \tag{15}$$

$$m_{v12}\ddot{z}_{12} - \sum_{u=1}^{2} v_{11u}(t) + \sum_{u=1}^{2} v_{12u}(t) = 0 \quad (16)$$

$$m_{v12}\lambda_{y1}^{2}\ddot{\theta}_{x12} - \sum_{u=1}^{2}(-1)^{u}\lambda_{y1}v_{11u}(t) + \sum_{u=1}^{2}(-1)^{u}\lambda_{y1}v_{12u}(t) = 0 \quad (17)$$

$$m_{v22}\ddot{z}_{22} - \sum_{u=1}^{2} v_{21u}(t) + \sum_{m=2}^{3}\sum_{u=1}^{2} v_{m2u}(t) = 0 \quad (18)$$

$$m_{v22}\lambda_{y3}^{2}\ddot{\theta}_{y22} + \sum_{m=2}^{3}\sum_{u=1}^{2}(-1)^{s}\lambda_{x3}v_{m2u}(t) = 0 \quad (19)$$

$$m_{v22}\lambda_{y2}^{2}\ddot{\theta}_{x22} - \sum_{u=1}^{2}(-1)^{u}\lambda_{y2}v_{21u}(t) + \sum_{u=2}^{3}\sum_{u=1}^{2}(-1)^{u}\lambda_{y2}v_{m2u}(t) = 0 \quad (20)$$

where,

$$\begin{aligned} v_{s1u}(t) &= k_{vs1u}\{z_{11} - (-1)^{s}\lambda_{ys1}\theta_{y11} \\ &+ (-1)^{u}\lambda_{xs1}\theta_{x11} - z_{s2} - (-1)^{u}\lambda_{xs2}\theta_{xs2}\} \\ &+ c_{vs1u}\{\dot{z}_{12} - (-1)^{s}\lambda_{sy1}\dot{\theta}_{y11} \\ &+ (-1)^{u}\lambda_{xs1}\lambda_{xs1}\dot{\theta}_{x11} - \dot{z}_{s2} - (-1)^{u}\lambda_{xs2}\dot{\theta}_{xs2}\} \end{aligned} \quad (21)$$

$$\begin{aligned} v_{12u}(t) &= k_{vs2u}\{z_{12} + (-1)^{u}\lambda_{x12}\theta_{x12} - z_{v1u}\} \\ &+ c_{vs2u}\{\dot{z}_{12} + (-1)^{u}\lambda_{x12}\dot{\theta}_{x12} - \dot{z}_{v1u}\} \end{aligned} \quad (22)$$

$$\begin{aligned} v_{m2u}(t) &= k_{vm2u}\{z_{22} + (-1)^{m}\lambda_{ym2}\theta_{y22}\} \\ &+ (-1)^{u}\lambda_{xm2}\theta_{x32} - z_{vm2}\} \\ &+ c_{vm2u}\{\dot{z}_{22} - (-1)^{m}\lambda_{ym2}\dot{\theta}_{y22} \\ &+ (-1)^{u}\lambda_{xm2}\dot{\theta}_{x32} - \dot{z}_{vm2}\} \end{aligned} \quad (23)$$

where, u=1 means left part of vehicle,
u=2 right part of vehicle,
m=2 Front tire on rear axle,
m=3 Rear tire on rear axle,
s=1 front axle and s=2 means rear axle.

The displacement of vehicle w_{vmu} that is in contact with road surface is affected by displacement of bridge $w(t, x_{mu})$ and road surface roughness $z_0(x_{mu})$, so that z_{vmu} can be expressed as Eq.(24):

$$z_{vmu} = w(t,x_{mu}) - z_0(t,x_{mu}) \quad (m=1,2,3) \quad (24)$$

where, m=1 ; Front tire
=2 ; Front tire of rear axle
=3 ; Rear tire of rear axle

The external force induced by the vehicle on bridge is expressed as Eq.(25):

$$[F] = \sum_{m=1}^{3}\varphi_{mu}P_{mu}(t) \quad (25)$$

where,

$\varphi_{mu}(t) = \{0 ; \cdots ; 0 ; \varphi_{k,mu} ; \varphi_{k+1,mu} ; \varphi_{k+2,mu} ; \varphi_{k+3,mu} ; 0 ; \cdots ; 0\}$

: load distribution vector to each node.

$P_{mu}(t)$: the contact force on front and rear axle of vehicle

A displacement $w(t,x_{mu})$ on the point contacted with road surface is,

$$w(t,x_{mu}) = \varphi_{mu}{}^{T}w = \varphi_{mu}{}^{T}\Phi a \quad (26)$$

where, Φ expresses modal matrix and a means a normal coordinate of displacement.

Contact force of vehicle is,

$$P_{mu}(t) = \frac{1}{2}(1-\frac{\lambda_{ys1}}{\lambda})m_{v}g + v_{m2u}(t) \quad (27)$$

where, g ; gravity

By substituting Eqs.(22) to Eq.(24) into Eq.(27), it is possible to set up the final formations of external force:

$$\begin{aligned} P_{1u}(t) &= \frac{1}{2}(1-\frac{\lambda_{y11}}{\lambda})m_{v}g \\ &+ k_{v12u}\{z_{12} - (-1)^{u}\lambda_{x12}\theta_{x12} - [\varphi_{1u}{}^{T}(t)\phi a - z_0(x_{1u})]\} \end{aligned} \quad (28)$$

$$+c_{v12u}\{\dot{z}_{12}-(-1)^u\lambda_{x12}\dot{\theta}_{x12}-[\varphi_{1u}{}^T(t)\dot{\phi}\dot{a}-\dot{z}_0(x_{1u})]\}$$

$$P_{mu}(t) = \frac{1}{2}(1-\frac{\lambda_{ym1}}{\lambda})m_v g + k_{vm2u}\{z_{22}+(-1)^m\lambda_{ym2}\theta_{y22}+(-1)^u\lambda_{x22}\theta_{x22} - [\phi_{mu}{}^T(t)\phi a - z_m(x_{mu})]\} + c_{vm2u}\{\dot{z}_{22}+(-1)^m\lambda_{ym2}\dot{\theta}_{y22}-(-1)^u\lambda_{x22}\dot{\theta}_{x22} + [\phi_{mu}{}^T(t)\phi\dot{a}-\dot{z}_0(x_{mu})]\} \quad (29)$$

In general, the forced vibration of bridge is expressed as Eq.(30). By substituting Eq.(25) into matrix [F] in Eq.(30), an equation of bridge-vehicle interaction is obtained as shown in Eq.(31). If an equation becomes to be uncoupled, at last it becomes the state that can be solved with ease. In order to get an uncoupled equation it is necessary to introduce concepts of normal coordinates. In Eq.(30), $w = \Phi_i\, a$ means a normal coordinate of displacement. It is possible to formulate an uncoupled equation as shown in Eq.(32) by substituting normalized displacement vector into Eq.(31) and multiplying both sides with Φ^T.

$$M_b\ddot{w} + C_b\,\dot{w} + K_b w = F$$

$$w = \sum_i \Phi_i a_i = \Phi a \quad (30)$$

$$M_b\ddot{w}+C_b\dot{w}+K_b w = \sum_{u=1}^{2}[\varphi^T{}_{1u}(t)\frac{1}{2}(1-\frac{\lambda_{y11}}{\lambda})m_v g + k_{v12u}\{z_{12}-(-1)^u\lambda_{x12}\theta_{x12}-[\varphi^T{}_{1u}(t)\Phi a - z_0(x_{1u})]\} + c_{v12u}\{\dot{z}_{12}-(-1)^u\lambda_{x12}\dot{\theta}_{x12}-[\varphi^T{}_{1u}(t)\Phi a-\dot{z}_0(x_{1u})]\}] + \sum_{m=2}^{3}\varphi^T{}_{su}(t)\frac{1}{2}(1-\frac{\lambda_{y12}}{\lambda})m_v g + k_{v12u}\{z_{22}+(-1)^s\lambda_{x12}\theta_{y22}+(-1)^u\lambda_{x12}\theta_{x12} - [\varphi^T{}_{mu}(t)\Phi a - z_0(x_{mu})]\} + c_{v12u}\{\dot{z}_{22}+(-1)^s\lambda_{x12}\dot{\theta}_{y22}+(-1)^u\lambda_{x12}\dot{\theta}_{x12} - [\varphi^T{}_{mu}(t)\Phi a-\dot{z}_0(x_{mu})]\} \quad (31)$$

The normalized equation of motion for bridge will become as follows:

$$\Phi^T M_b\Phi\ddot{a} + \Phi^T C_b\Phi\dot{a} + \Phi^T M_b\Phi a - \sum_{m=1}^{3}\sum_{u=1}^{2}\Phi^T\varphi_{mu}(t)[k_{vmu}\varphi^T{}_{mu}(t)\Phi a + c_{vmu}\,\varphi^T{}_{mu}(t)\Phi\dot{a}] - \sum_{u=1}^{2}[\Phi^T\varphi_{1u}(t)[k_{v12u}\{-z_{12}-(-1)^u\lambda_{x12}\theta_{x12}\} + c_{v12u}\{-\dot{z}_{12}-(-1)^u\lambda_{x12}\theta_{x12}\} + \sum_{m=1}^{3}[\Phi^T\varphi_{mu}(t)[k_{vm2u}\{z_{22}+(-1)^m\lambda_{ym2}\theta_{y22} - (-1)^u\lambda_{x22}\theta_{x22}\} + c_{vm2u}\{\dot{z}_{22}+(-1)^m\lambda_{ym2}\dot{\theta}_{y22} - (-1)^u\lambda_{x22}\dot{\theta}_{x22}\}] = \sum_{u=1}^{2}\Phi^T\varphi_{1u}(t)[\frac{1}{2}(1-\frac{\lambda_{y11}}{\lambda})m_v g + \sum_{u=1}^{2}\sum_{m=2}^{3}\Phi^T\varphi_{mu}(t)[\frac{1}{2}(1-\frac{\lambda_{ym1}}{\lambda})m_v g] + \sum_{m=1}^{3}\sum_{u=1}^{2}\Phi^T\varphi_{mu}(t)\{k_{vm2u}z_0(x_{mu})+c_{vm2u}\dot{z}(x_{mu})\} \quad (32)$$

Equation (32) expresses the equation of forced vibration of bridge and it contains variables which are related to vehicle motion. The normalized equation of motion about vehicle can be acquired by substituting Eq.(21)~(24) into Eq.(13)~(20). The final normalized equations of motion about 8-degree-of-freedom vehicle model become as shown in Eqs.(33) to (40):

$$m_{v11}\,\ddot{z}_{11} + \sum_{s=1}^{2}\sum_{u=1}^{2}[k_{vs1u}\{z_{11}-(-1)^s\lambda_{ys1}\theta_{y11} + (-1)^u\lambda_{xs1}\theta_{x11}-z_{s2}-(-1)^u\lambda_{xs2}\theta_{xs2}\} + c_{vs1u}\{\dot{z}_{12}-(-1)^s\lambda_{ys1}\dot{\theta}_{x11}+(-1)^u\lambda_{xs1}\dot{\theta}_{x11} - \dot{z}_{s2}-(-1)^u\lambda_{xs2}\dot{\theta}_{xs2}\}] = 0 \quad (33)$$

$$m_{v11}\,\gamma_{y1}{}^2\,\ddot{\theta}_{y11} \tag{34}$$
$$-\sum_{s=1}^{2}\sum_{u=1}^{2}(-1)^s\lambda_{ys1}[k_{vs1u}\{z_{11}-(-1)^s\lambda_{ys1}\theta_{y11}$$
$$+(-1)^u\lambda_{xs1}\theta_{x11}-z_{s2}-(-1)^u\lambda_{xs2}\theta_{xs2}\}$$
$$+c_{vs1u}\{\dot{z}_{12}-(-1)^s\lambda_{ys1}\dot{\theta}_{x11}+(-1)^u\lambda_{xs1}\dot{\theta}_{x11}$$
$$-\dot{z}_{s2}-(-1)^u\lambda_{xs2}\dot{\theta}_{xs2}\}]=0$$

$$m_{v11}\,\gamma_{x1}{}^2\,\ddot{\theta}_{x11} \tag{35}$$
$$-\sum_{s=1}^{2}\sum_{u=1}^{2}(-1)^u\lambda_{x11}[k_{vs1u}\{z_{11}-(-1)^s\lambda_{ys1}\theta_{y11}$$
$$+(-1)^u\lambda_{xs1}\theta_{x11}-z_{s2}-(-1)^u\lambda_{xs2}\theta_{xs2}\}$$
$$+c_{vs1u}\{\dot{z}_{12}-(-1)^s\lambda_{jys1}\dot{\theta}_{x11}+(-1)^u\lambda_{xs1}\dot{\theta}_{x11}$$
$$-\dot{z}_{s2}-(-1)^u\lambda_{xs2}\dot{\theta}_{xs2}\}]=0$$

$$-\sum_{u=1}^{2}[k_{v12u}\varphi^T{}_{1u}(t)\Phi a+c_{v12u}\varphi^T{}_{1u}(t)\Phi\dot{a}]$$
$$+m_{v12}\ddot{z}_{12}-\sum_{u=1}^{2}[k_{v11u}\{z_{11}+\lambda_{y11}\theta_{y11}+(-1)^u\lambda_{x11}\theta_{x11}$$
$$-z_{12}-(-1)^u\lambda_{x12}\theta_{x12}\}+c_{v11u}\{\dot{z}_{11}+\lambda_{y11}\dot{\theta}_{y11}$$
$$+(-1)^u\lambda_{x11}\dot{\theta}_{x11}-\dot{z}_{12}-(-1)^u\lambda_{x12}\dot{\theta}_{x12}\}] \tag{36}$$
$$-\sum_{u=1}^{2}[k_{v12u}\{z_{12}+(-1)^u\lambda_{x12}\theta_{x12}\}$$
$$+c_{v12u}\{\dot{z}_{12}+(-1)^u\lambda_{x12}\dot{\theta}_{x12}\}]$$
$$=\sum_{u=1}^{2}[-k_{v12u}z_0(x_{1u})-c_{v12u}\,\dot{z}_0(x_{1u})]$$

$$-\sum_{u=1}^{2}(-1)^u\lambda_{x12}\{k_{v12u}\varphi^T{}_{1u}(t)\Phi a$$
$$+c_{v12u}\varphi^T{}_{1u}(t)\Phi\dot{a}\}+m_{v12}\gamma^2{}_{x2}\,\ddot{\theta}_{x12}$$
$$-\sum_{u=1}^{2}(-1)^u\lambda_{x12}[k_{v11u}\{z_{11}+\lambda_{y11}\theta_{y11}$$
$$+(-1)^u\lambda_{x11}\theta_{x11}-z_{12}-(-1)^u\lambda_{x12}\theta_{x12}\} \tag{37}$$
$$+c_{v11u}\{\dot{z}_{11}+\lambda_{y11}\,\dot{\theta}_{y11}+(-1)_u\lambda_{x11}\dot{\theta}_{x11}$$
$$-\dot{z}_{12}-(-1)^u\lambda_{x12}\dot{\theta}_{x12}\}]$$
$$+\sum_{u=1}^{2}(-1)^u\lambda_{x12}[k_{v12u}\{z_{12}+(-1)^u\lambda_{x12}\theta_{x12}\}$$
$$+c_{v12u}\{\dot{z}_{12}+(-1)^u\lambda_{x1}\dot{\theta}_{x12}$$
$$=-\sum_{u=1}^{2}(-1)^u\lambda_{x12}[k_{v12u}z_0(x_{1u})+c_{v12u}\,\dot{z}(x_{1u})]$$

$$-\sum_{m=2}^{3}\sum_{u=1}^{2}[k_{vm2u}\,\varphi^T{}_{su}(t)\Phi a+c_{vm2u}\varphi^T{}_{mu}(t)\Phi\dot{a}]$$
$$+m_{v22}\,\ddot{z}_{22} \tag{38}$$
$$-\sum_{u=1}^{2}[k_{v21u}\{z_{11}-\lambda_{y21}\theta_{y11}+(-1)^u\lambda_{x11}\theta_{x11}$$
$$-z_{22}-(-1)^u\lambda_{x22}\theta_{x22}\}-c_{v21u}\{\dot{z}_{11}-\lambda_{y21}\dot{\theta}_{y11}$$
$$+(-1)^u\lambda_{x11}\dot{\theta}_{x11}-\dot{z}_{22}-(-1)^u\lambda_{x22}\dot{\theta}_{x22}\}]$$
$$+\sum_{m=2}^{3}\sum_{u=1}^{2}[k_{vm2u}\{z_{22}+(-1)^m\lambda_{ym2}\theta_{y22}+(-1)^u\lambda_{x22}\theta_{x22}\}$$
$$+c_{vm2u}\{\dot{z}_{22}+(-1)^m\lambda_{ym2}\dot{\theta}_{y22}+(-1)^u\lambda_{x22}\dot{\theta}_{x22}\}]$$
$$=\sum_{m=2}^{3}\sum_{u=1}^{2}[-k_{vm2u}z_0(x_{mu})-c_{vm2u}\dot{z}(x_{mu})]$$

$$-\sum_{m=2}^{3}\sum_{u=1}^{2}(-1)^m\lambda_{ym2}[k_{vm2u}\varphi^T{}_{mu}\Phi a+c_{v2u}\varphi^T\Phi\dot{a}]$$
$$+m_{22}\,\gamma^2{}_{y2}\,\ddot{\theta}_{y22} \tag{39}$$
$$-\sum_{m=2}^{3}\sum_{u=1}^{2}(-1)^m\lambda_{ys2}[k_{vm2u}\{z_{22}+(-1)^m\lambda_{ym2}\theta_{y22}$$
$$+(-1)^u\lambda_{xm2}\theta_{x32}\}+c_{vm2u}\{\dot{z}_{22}+(-1)^m\lambda_{ym2}\theta_{y22}$$
$$+(-1)^u\lambda_{xm2}\theta_{x32}$$
$$=-\sum_{m=2}^{3}\sum_{u=1}^{2}(-1)^m\lambda_{ym2}[k_{vm2u}z_0(x_{mu})+c_{v2u}\dot{z}_0(x_{mu})]$$

$$-\sum_{m=2}^{3}\sum_{u=1}^{2}(-1)^u\lambda_{x22}[k_{vm2u}\varphi^T{}_{mu}(t)\Phi a$$
$$+c_{vm2u}\varphi^T{}_{mu}(t)\Phi\dot{a}]+m_{v22}\gamma^2{}_{x22}\ddot{\theta}_{x22}$$
$$-\sum_{u=1}^{2}(-1)^u\lambda_{x22}[k_{v21u}\{z_{11}-\lambda_{y21}\theta_{y11}+(-1)^u\lambda_{x11}\theta_{x11}$$
$$-z_{22}-(-1)^u\lambda_{x22}\theta_{x22}\} \tag{40}$$
$$-\dot{z}_{22}-(-1)^u\lambda_{x22}\dot{\theta}_{x22}\}]$$
$$+\sum_{m=2}^{3}\sum_{u=1}^{2}(-1)^u\lambda_{x22}[k_{vm2u}\{z_{22}+(-1)^m\lambda_{ym2}\theta_{y22}$$
$$+(-1)^u\lambda_{x22}\theta_{x22}\}$$

$$+c_{vm2u}\{\dot{z}_{22}+(-1)^m\lambda_{ym2}\dot{\theta}_{y22}+(-1)^u\lambda_{x22}\dot{\theta}_{x22}\}]$$
$$=\sum_{m=2}^{3}\sum_{u=1}^{2}(-1)^u\lambda_{x22}[-k_{vm2u}z_0(x_{mu})-c_{vm2u}\dot{z}(x_{mu})]$$

where, Equation (33) expresses the bouncing of vehicle, Eq.(34) pitching, Eq.(35) rolling, Eq. (36) parallel hop of front axle, Eq.(37) tramp of front axle, Eq.(38) parallel hop of rear axle, Eq.(39) axle windup and Eq.(40) expresses tramp of rear axle. Equations (32) to (40) are the final simultaneous equations of motion due to the traffic-induced loading, and of course these equations include the terms of road surface roughness.

4. Numerical analysis

4.1 Generated road surface model[4,6]

In this paper, the power spectrum of road surface profile is assumed as Eq.(41).[4] By using this equation, a road profile model which is assumed to be stationary random process is generated by means of Monte Carlo method.

$$S_z(\Omega)=\frac{\alpha}{\Omega^n+\beta^n} \tag{41}$$

where, α ; spectral roughness coefficient,
β ; spectral shape coefficient,
Ω ; roughness frequency,
n ; spectral roughness exponent.

As sampling function of road profile, the following Eq.(42)[6] is to be manipulated.

$$z_r(x)=\sum_{k=1}^{M}\alpha_k\sin(\omega_k x+\varphi_k) \tag{42}$$

where,

a_k : Gaussian random variable having zero mean value and variance as $\sigma_k^2=4S_r(\Omega_k)\Delta\Omega$

Ω_k : the space frequency of road surface roughness when vehicle velocity is V, which may be also stated as

$\omega_k=2\pi V\Omega_k$,

$\Omega_k=\Omega_L+(k-\frac{1}{2})\Delta\Omega$,

$\Delta\Omega=(\Omega_u-\Omega_L)/M$

Ω_L : the smallest limit of frequency,

Ω_u : the largest upper limit of frequency,

M : an integer number that is large enough,

φ_k : a random variable having constant distribution within $0\sim2\pi$ and

$S_r(\Omega_k)$: Power spectral density of road surface roughness.

To generate a random road surface profile, first of all random numbers between 0 and 1 should be generated by using computer. Then

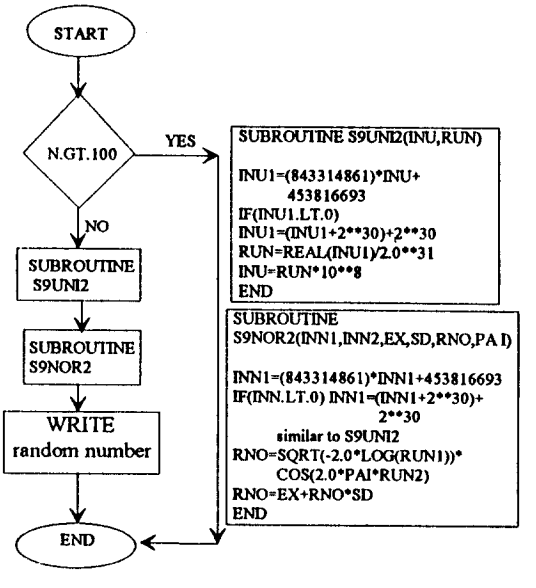

FIG. 3 Flow chart of generating random numbers

by using these random numbers, artificial road surface profile that satisfies the assumptions are obtained. The following flow chart (Fig.3) shows the process of generating random values by 32-bit computer. Of course, the values used in this flow chart should be changed in case of applying other types of computer. Figure 4 shows the profile and power spectral density(P. S. D.) of measured road surface on test bridge (Umeda enterance of Hanshin express way in Osaka, Japan). The straight lines on P. S. D. of Fig.4 indicates the boundaries of ISO standard[3] which estimates roadway roughness based on the riding comfort of vehicle. By using ISO, it can be seen that the condition of measured road surface may be categorized as 'Extra Good'.

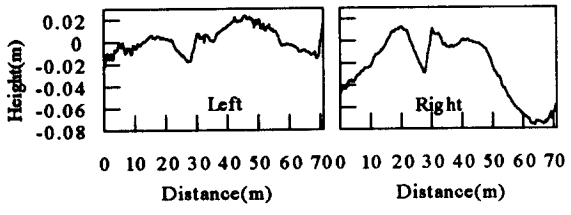

(a) Measured Road Surface Profile

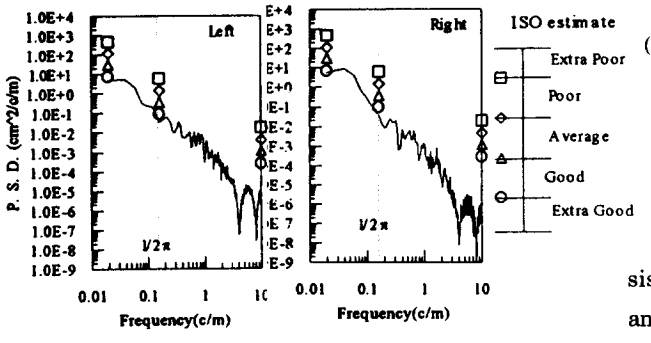

(b) P.S.D. of surface roughness and ISO categories(Extra Good condition)

FIG. 4 Measured road profile and P.S.D. on test bridge

Figure 5 shows the generated road surface profile and its power spectral density that is generated by using $\alpha=0.003(cm^2/\ m/\ cycle)$, $\beta=0.02(cycle/m)$ and $n=2.5$ based on the concept of Eq.(41), and generated frequency range adopted in Fig.5 is 0.01(cycle/m) to 3.0(cycle/m). The random road roughness generated using above three factors would go into boundary called as 'Good state' specified by ISO.

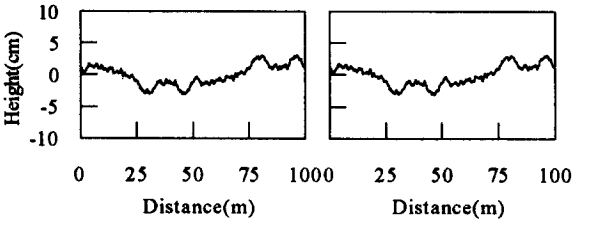

(a) Generated road Profile generated(0.01~3(c/m))

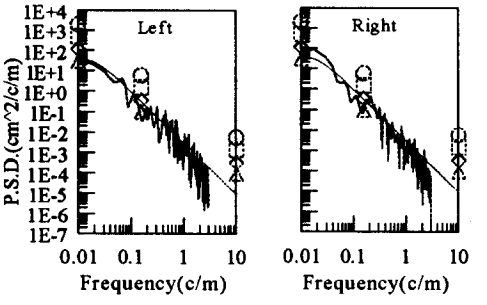

(b) P.S.D. of generated surface roughness and ISO categories
($\alpha=0.003$, $\beta=0.02$ and $n=2.5$: Good condition)

FIG. 5 Generated road profile and P.S.D.

4.2 Bridge and vehicle model

The bridge adopted in experiment and analysis is a steel girder bridge as shown in Fig.6 and the structural properties are shown in Table 1. In analysis, to account the torsional properties more accurately, the stiffness of guardrail is considered. The locations to be analyzed are the same as those of testing point. The characteristics and dimensions of vehicle

used in experiment and analysis are shown in Fig.7 and Table 2.

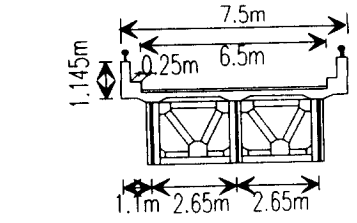

(a) Cross section of bridge model

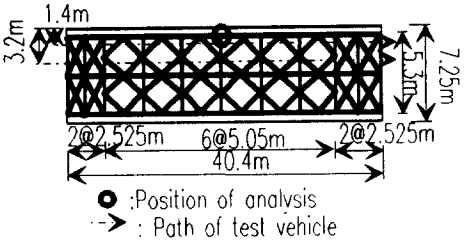

(b) General view of model

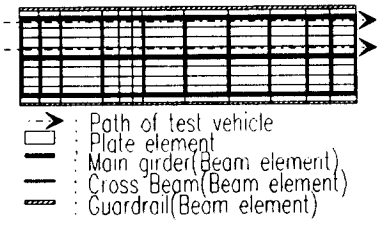

(c) F. E. M. model

FIG. 6 Test and analytical bridge model

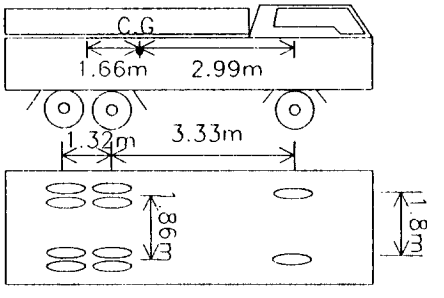

FIG. 7 Testing Vehicle

Table 1 Properties of Test bridge

Type	I-shaped composite plate girder
Class	First class
Span length(m)	40.4
Width(m)	7.5
Effective Width(m)	6.5
Deck plate	Reinforced concrete slab (t=17cm)
Girders	3-girders
Weight per unit length(kg/m)	7.706×10^{2}
Ratio of young's modulus	9.516
Ratio of shear modulus	8.565
Area of section of girder (m^2)	0.1415
Moment of inertia of girder(m^4)	0.2122
Torsional constant(m^4)	0.3843×10^{-1}
Warping constant(m^6)	0.79
Damping constant for 1-st and 2-nd modes	0.02

Table 2 Constants of Test Vehicle

Vehicle Type			3-axled dump truck (rear tandem)
Total Weight(ton)			19.47
Weight of tire (ton)	Front		0.25
	Rear		0.1875
Spring constant (t/m)	suspension	Front	161
		Rear	482
	Front tire		321
	Rear tire		482
Damping constant (t·s/m)	suspension	Front	1.14
		Rear	3.41
	Front tire		1.36
	Rear tire		1.02

4.3 The results of numerical analysis

The aims of this numerical analysis are to verify the analytical model by comparing experimental results of actual vehicle and bridge. In addition, the response and dynamic incremental factor (D. I. F) of bridge under several speed conditions and road roughness are examined.

4.3.1 Effect of vehicle and its speed to bridges

Generally the natural frequencies of girder system are similar to those of vehicle body. The power spectrums of vehicle body and tire by experiment are shown in Fig.8. Figure 9 shows the analyzed power spectrum of vehicle Body and tire. Form Figures 8 and 9 it can be seen that the vibration characteristics of analytical vehicle model are well fitted to those of experiment. The tested and analyzed natural frequencies of bridge and vehicle are shown in Table 3. Table 3 shows that the natural frequency of bridge girder system is similar to that of vehicle body, therefore it can be seen

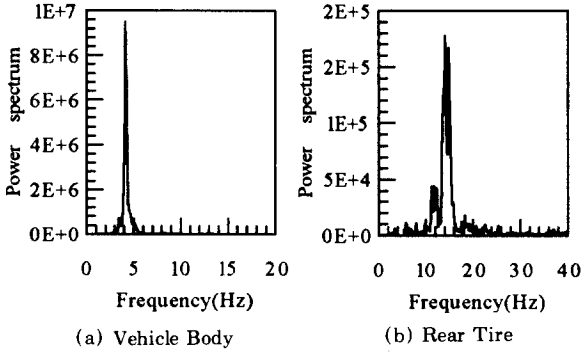

(a) Vehicle Body (b) Rear Tire

FIG. 8 Power spectrum of acceleration by experiment

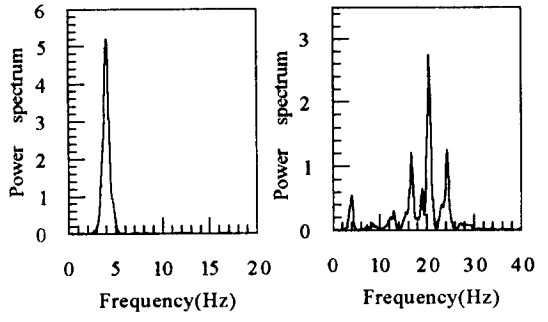

(a) Vehicle body (b) Rear Tire

FIG. 9 Power spectrum of acceleration by analysis

Table 3 Natural frequencies of the test vehicle and bridge.

Class		Frequency (Hz)	
		Analysis	Experiment
Test Vehicle	Body	4.0	5.0
	Tire	19.5	17.5
Girder Bridge	1st (Bending)	2.35	2.33
	2nd (Torsion)	3.86	3.86
	3rd (Bending)	9.42	–

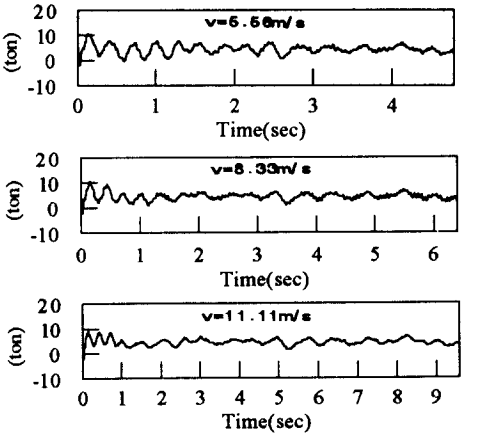

FIG. 10 Contact forces of vehicle at different speed by analysis
(Road surface condition $\alpha=0.003$, $\beta=0.02$ and $n=2.5$)

that dynamic response of girder bridge is affected by dynamic behavior of vehicle body. In addition, Figure 10 shows the contact force of vehicle by analysis, and from this figure it can also be seen that contact force of vehicle varies with vehicle speed.

The parametric studies on dynamic response of a bridge due to a moving vehicle is estimated by using the concept of D. I. F.[7] The concept of D. I. F. used in this study expresses the ratio of dynamic amplitude to the maximum static response, and Figure 11 shows a general idea of D. I. F. In Fig.11 $Y_{s,max}$ expresses the

maximum static response and $|Y_d - Y_s|$ denotes the maximum absolute difference between dynamic and static responses during one major period of the dynamic response including $Y_{s,max}$.

Figure 12 shows the variations of D. I. F. according to vehicle speed, and Fig.13 shows the time histories of bridge due to different vehicle speed running on the same artificial road surface by analysis. From figures 12 and 13, it can be seen that dynamic response does not always increase with vehicle speed. This tendency with vehicle speed is similar to the variation of contact forces shown in Fig. 10.

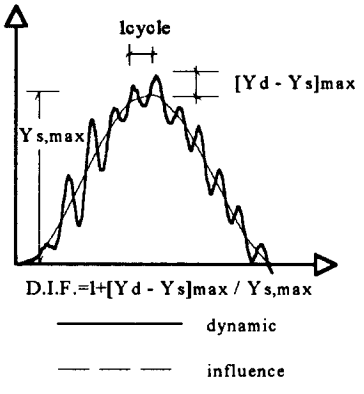

FIG. 11 Definition of D.I.F.

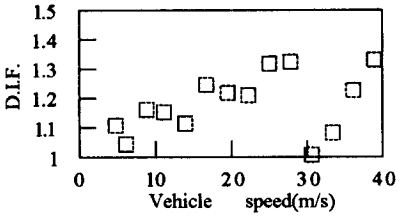

FIG. 12 D.I.F. according to vehicle speed
(Road surface condition $\alpha=0.003$, $\beta=0.02$ and $n=2.5$)

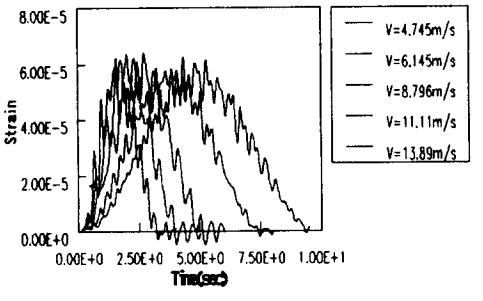

FIG. 13 Time histories of bridge with vehicle speed
(Road surface condition $\alpha=0.003$, $\beta=0.02$ and $n=2.5$)

4.3.2 Effect of road surface roughness

The effect of road roughness to bridge and vehicle responses can be prospected easily with common sense. However, the point of view taken in this paper about the road roughness certifies how does a theoretical model matches with that of the measured road surface.

Figure 14 shows the time histories of bridge due to artificial road surface profile according to different road condition defined by α at vehicle speed 4.745m/s. In this figure, the used road conditions are $\alpha=0.003$, $\alpha=0.01$ and $\alpha=0.03$, and these factors means the condition of road surface categorized as 'Good', 'Average' and 'Poor' respectively in ISO standard.

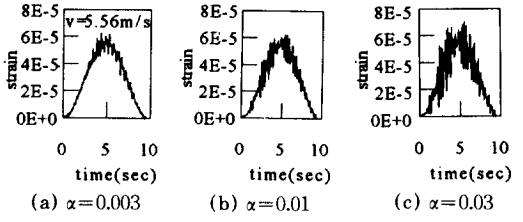

FIG. 14 Time histories of bridge by different road surface($\beta=0.02$ and $n=2.5$ in all cases)

In Fig.15, it shows D. I. F. of bridge due to different road surface conditions like as used in Fig.14. From this figure it can be seen that dynamic response of bridge is affected by road surface condition severely, therefore it is necessary to consider the effect of road surface condition in estimating impact factor.

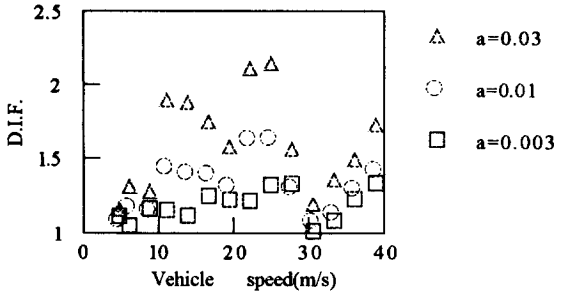

FIG. 15 D.I.F. vs. Vehicle speed due to different road surface conditions

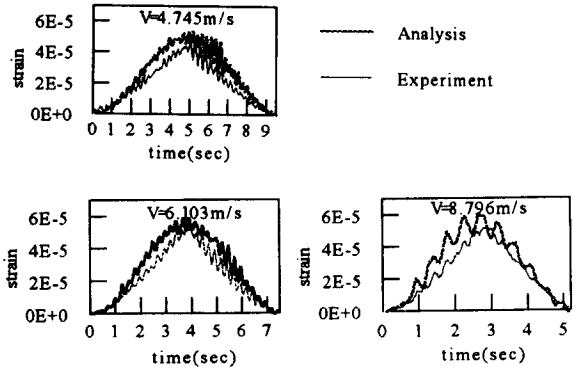

FIG. 16 Time history of dynamic response at center of external girder
(By using measured surface as shown in FIG. 4)

Figure 16 shows the time histories of girder at center of external girder as shown in Fig. 6 (b), and Fig.17 shows those of deck slab at the location marked by circle in Fig. 6 (c) due to vehicle running on measured road surface as shown in Fig.4(a). These time histories of experiment and analysis in Fig.16 are well fitted at each other. However in the case of concrete deck slab, those are not well fitted each other. This may be the reason that in the case of concrete estimation of material properties is more difficult than that of steel. From those results, the analytical model used in this study can be used in practice.

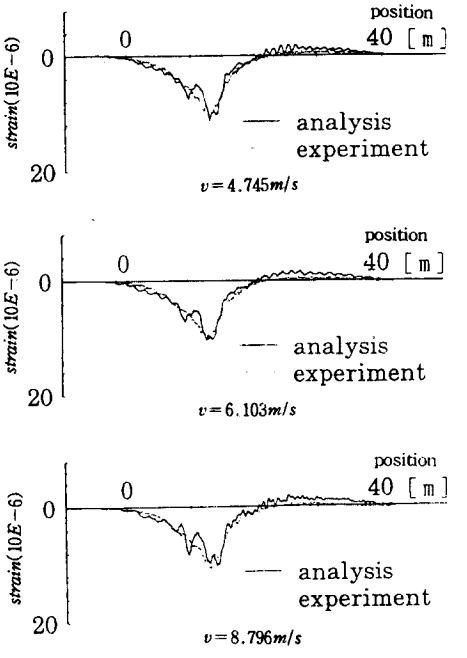

FIG. 17 Time histories of deck plate of birdge model
(By using measured surface as shown in FIG. 4)

5. Conclusions and future works

The objective of this research is to develope a computer program to solve dynamic problem of bridge that include 8-degree-of-vehicle model and road surface roughness. From the analytical and experimental results we can summarize remarks as follows ;

1) The analyzed dynamic characteristic of vehicle has been well fitted to the experimental results through spectral analysis, which means the numerical model may be used in practice.

2) The analytical time histories of girder are similar to those of experiment, however in the case of deck plate those are not well fitted each other. These difference in deck slab may come from the incorrectness of estimating properties of concrete.

3) From the natural frequencies of vehicle and girder, it is easy to understand that the dynamic response of girder is mainly affected by motion of vehicle body.

4) We can see that artificial road data may be used in practice, provided that we may be able to assume appropriate values of α, β and n. To assume these values correctly, much experience which can be acquired by actual affairs on analyzing real or measured road profile data is required.

From the small numbers of parametric study as done in this paper, it is not clear to find out the influence of vehicle speed to dynamic behavior of bridge. However, in Fig.15 we can see the possibilities that the difference of D. I. F. between different road condition become large according to vehicle speed. This phenomenon is similar to the effect of gap heights at expansion joint on bridge which has been studied in reference(9).

To take a further step from this research, we will carry out the parametric analysis of bridges due to various vehicle speed on the many different span length with faultings at expansion joints accompanied with the research about behavior of vehicle by using the program developed in this research.

References

1. Honda, H, Kajikawa, Y. and Kobori, T., 'Spectra of Road Surface Roughness on Bridge', ASCE, Vol.108, No.ST9, pp1956-1966, September, 1982.
2. Kaneshige, I., 'Analysis of Road Surface Roughness', Isuzu Technical Journal, No.50, pp.1-7 1967. (in Japanese)
3. ISO; Proposals for Generalized Road Inputs to Vehicles, ISO/DIS 2631, pp.1-7, 1972.
4. Kawatani, M., Komatsu. S. and Sasaki, T., Proc., JSCE, No.3921/I-9, 351, 1988. (in Japanese)
5. Agabein, M. E., 'The Effect of Various Damping Assumptions on the Dynamic Response of Structures', Bulletin of International Institute of Seismology and Earthquake Eng. Vol.8, pp. 217-236, 1971.
6. Hoshiya, M., 'Dynamic Analysis by Random Process', Kashima Press Co. pp.46-58, 1974. (in Japanese)
7. Kawatani, M., Nishiyama, S. and Yamada, Y., ' Dynamic Response Analysis of Highway Bridges under Moving Vehicle', Technical Reports of the OSAKA University, Vol.43, No.2137, pp. 109-118, April, 1993.
8. Kim, C. W. and Kawatani, M., 'Three - Dimensional Dynamic Response Analysis of Highway Bridge under Moving Vehicle on Random Road Profile', 4th Japan-Korea Joint Seminar on Steel Bridges, December, 1996. Osaka, Japan.
9. Structure Division, Structure and Bridge Department, Public Works Research Institute, Ministry of Construction of Japan 'Experimental Research on Live Loads for Bridge Design', Technical Report, VII-1985, Materials of Research Institute, No.2258, December, 1985. (in Japanese)